Published in final edited form as:
Arthritis Rheum. 2010 August ; 62(8): 2370–2381. doi:10.1002/art.27512.

MMP-13 loss associated with impaired ECM remodelling disrupts chondrocyte differentiation by concerted effects on multiple regulatory factors

Rosa Maria Borzi[1,*,#], **Eleonora Olivotto**[1,#], **Stefania Pagani**[1], **Roberta Vitellozzi**[1], **Simona Neri**[1], **Michela Battistelli**[2], **Elisabetta Falcieri**[2], **Annalisa Facchini**[3], **Flavio Flamigni**[3], **Marianna Penzo**[4,5], **Daniela Platano**[1], **Spartaco Santi**[6], **Andrea Facchini**[1,7], and **Kenneth B Marcu**[1,8,*]

[1] Laboratorio di Immunoreumatologia e Rigenerazione Tissutale, Istituti Ortopedici Rizzoli, Via di Barbiano 1/10, Bologna, Italy

[2] Istituto di Scienze Morfologiche, Università degli Studi “Carlo Bo”, Urbino, Italy

[3] Dipartimento di Biochimica, Università degli Studi di Bologna, Bologna, Italy

[4] Vita Salute San Raffaele University, Via Olgettina 58, 20132 Milano, Italy

[5] Centro Ricerca Biomedica Applicata (CRBA), Policlinico S. Orsola-Malpighi, via Massarenti 9, Bologna, Italy

[6] Istituto di Genetica Molecolare CNR, Bologna, Italy

[7] Dipartimento di Medicina Clinica, Università degli Studi di Bologna, Bologna, Italy

[8] Dept. of Biochemistry and Cell Biology, Stony Brook University, Stony Brook, NY, 11794-5215 USA

Abstract

Purpose—To link MMP-13 activity and ECM remodeling to alterations in regulatory factors leading to a disruption in chondrocyte homeostasis.

Methods—Matrix-metalloproteinase-13 (MMP-13) expression was ablated in primary human chondrocytes by stable retrotransduction of short-hairpin RNAs. The effects of MMP-13 KD on key regulators of chondrocyte differentiation (Sox9, Runx2 and β-catenin), and angiogenesis (VEGF) were scored at the protein (immunohistochemistry or western blot) and RNA (real time PCR) levels in high density monolayer and micromass cultures under mineralizing conditions. Effects on cellular viability in conjunction with chondrocyte progression towards a hypertrophic-like state were assessed in micromass cultures. Alterations in Sox9 subcellular distribution were assessed by confocal microscopy in micromass cultures and also in OA cartilage.

Results—Differentiation of control chondrocyte micromasses progressed up to a terminal phase, with calcium deposition in conjunction with reduced cell viability and scant ECM. MMP-13 knock-down (KD) impaired ECM remodeling and suppressed differentiation in conjunction with reduced levels of Runx2, β-catenin and VEGF. MMP-13 levels *in vitro* and ECM remodeling *in vitro* and *in vivo* were linked to changes in Sox9 sub-cellular localization. Sox9 was largely excluded from the nuclei of chondrocytes with MMP-13 remodeled or degraded ECM, and

[*]Corresponding authors: Dr. Rosa Maria Borzi, Laboratorio di Immunologia e Genetica, Istituti Ortopedici Rizzoli, via di Barbiano 1/10, 40136, Bologna, Italy, rosamaria.borzi@ior.it; Telephone: +39-051-6366803, Fax: +39-051-6366807. and Prof. Kenneth B. Marcu: kenneth.marcu@unibo.it;.
[#]These authors contributed equally to this work

exhibited an intranuclear staining pattern in chondrocytes with impaired MMP-13 activity *in vitro* or with more intact ECM *in vivo*.

Conclusions—MMP-13 loss leads to a break-down in primary human articular chondrocyte differentiation by altering the expression of multiple regulatory factors.

Keywords

MMP-13; ECM remodeling; osteoarthritis; differentiation; shRNA retrovirus

Introduction

Chondrocyte maturation is arrested in articular cartilage, which prevents their differentiation towards a more terminal hypertrophic-like phenotype (1). The mechanisms maintaining articular chondrocyte (AC) homeostasis are perturbed in osteoarthritis (OA), wherein chondrocytes recapitulate aspects of endochondral ossification, which is driven by changes in ECM synthesis and remodelling in conjunction with an angiogenic switch (1). Although expression of type X collagen (Col10) and MMP-13 by ACs in OA are markers of this abnormal phenotype, our understanding of what precisely re-triggers chondrocyte differentiation in OA disease remains scant.

MMPs are not only the effectors of ECM remodeling but also act as an initiating force leading to endochondral ossification (2), vascular invasion, altered bioavailability of growth factors and chondrocyte apoptosis. For instance, MMP activity cleaves chemokines into activated forms and incapacitates angiogenesis inhibitors, thereby altering the chemotactic and angiogenic environment. Recent studies with mice lacking specific MMPs have revealed their roles in endochondral bone development. MMP-13 is the major collagenase expressed at primary and secondary ossification centers (2,3); and it drives endochondral ossification due to its catalytic activity on major *in vivo* substrates like collagen II (Col2) and aggrecan (2,4), The latter two proteins are the principle constituents of normal articular cartilage, a tissue programmed to remain in a maturation arrested state. However, this homeostasis is dramatically perturbed by severe cartilage degradation in OA with ECM remodeling compromising cartilage function as a consequence of lost ECM proteins and cell anoikis (5). Thus, targeting MMP-13 in OA disease could maintain tissue homeostasis (6), prevent unwanted vascularization and perhaps even help to re-establish AC maturation arrest.

ACs show “phenotypic plasticity” *in vitro* and in differentiating micromass cultures recapitulate aspects of their normal differentiation programming by converting to a hypertrophic-like state (7). Osteogenic additives are dispensable in OA chondrocyte micromasses perhaps due to their intrinsic commitment towards a hypertrophic-like state, as exemplified by their enhanced degree of ECM remodelling (8).

In prior work, we showed that IKKα ablation in ACs stabilized their ECM by post-transcriptionally suppressing MMP-13 activity, thereby blocking their differentiation and maintaining them in an early peri-articular-like state (8). Here we show that MMP-13 loss alone impedes the differentiation of primary chondrocyte micromasses by inhibiting the expression or activation of multiple regulatory factors including Runx2**,** VEGF and β-catenin. Moreover, we also find that the latter effects of impaired MMP-13 activity in chondrocyte micromasses are associated with enhanced nuclear localization of Sox9. Taken together our data suggest that MMP-13 facilitates chondrocyte terminal differentiation by ensuring the concerted up-regulation of Runx2, VEGF and active β-catenin.

Materials and Methods

Stable MMP-13 knock-down in primary chondrocytes

With local Ethics Committee approval, primary chondrocytes from 16 OA patients undergoing knee arthroplasty, were stably transduced with pSuper retroviral vectors (OligoEngine Inc.) harbouring MMP-13 specific shOligos. In most cases, MMP-13 KDs of ACs from different patients were generated with two different shOligos targeted to different MMP-13 exons (NM_002427): OE7 (538–554 nt) and OE 16 (1399–1417 nt). Control chondrocytes were stably transduced with a GL2 luciferase shOligo retrovector retroviral vector (8). MMP-13 KDs were verified by real time PCR and Elisa assays of cell supernatants. IKKα KD and IKKβ KD chondrocytes were prepared as described (8).

Real time PCR analysis

Real Time PCRs were done as previously described (8) with Forward (F) and reverse (R) PCR primers including: GAPDH (NM_002046) 579–598F and 701–683R); MMP-13 (NM_002427), 496–511F and 772–756R; Sox-9 (NM_000346) 952–968F and 1069–1054R; Runx2 variant transcript 3 (NM_004348) 864–883F and 968–949R; Runx2 variant transcripts 2 (NM_001015051) and 1 (NM_001024630) 716–735F and 820–801R; β-catenin (NM_001904) 1031–1052F and 1313–1293R; VEGF variant transcripts 7 (NM_001033756.1), 6 (NM_001025370.1), 5 (NM_001025369.1), 4 (NM_001025368.1), 3 (NM_001025367.1), 2 (NM_003376.4), and 1 (NM_001025366.1) 1144–1126F and 1063–1079R). Primers were annealed at 56°C, except Sox9, was at 60°C.

MMP-13 ELISA Assays

MMP-13 protein secreted after 72 hours was quantified by ELISA (5,8). MMP-13 KD efficiencies were assessed in triplicate with adherent cells that had re-established their ECM. Cells were either untreated or IL-1β (100 U/ml) stimulated. Micromass cultures were either untreated or stimulated with 100 U/ml IL-1β, 100 nM CXCL13/BCA-1, 100 nM CXCL12/SDF-1α, CCL20/Larc or 100 nM CXCL1/GRO.

Micromass culture and analysis

Cells were seeded into micromass cultures as previously described (5,8).

Quantitative glycosaminoglycan (GAG) analysis

Glycosaminoglycan (GAG) content of micromasses were quantified by the dimethylmetilen blue assay as described (8).

Collagen C1,2C neo-epitope ELISA

Collagen 2 (Col2) neo-epitopes (Col2-3/4C short or C1,2C), the carboxy terminus of the ¾ peptide generated by “rate limiting” collagenases 1, 8 and 13, were quantified by ELISA (Ibex Pharmaceuticals, Mont Royal, QC).

Immunohistochemistry

Micromasses were prepared and analyzed by IHC along with Hematoxylin counterstaining of nuclei as previously described (8). Col2, Col 2-3/4C neo-epitopes, Runx2 and Col10 were analyzed essentially as described (8). VEGF expression was detected, without prior antigen unmasking, with mouse monoclonal anti-human VEGF antibody (R&D, Minneapolis, MN). Sox9 expression was evaluated after antigen unmasking with a goat polyclonal antiserum (R&D). β-catenin IHC was done with a goat polyclonal anti-β-catenin antibody (R&D) and active β-catenin dephosphorylated on Ser37 or Thr41 was detected with a mouse

monoclonal antibody (Upstate, Lake Placid, N. Y). Sox9 levels in maturing micromasses were quantified with 4–5 non-overlapping images from multiple slides, which were obtained with a Nikon Eclipse 90i microscope equipped with NIS (Nikon Imaging Software) elements (Nikon Inc) as previously described (8).

Transmission electron microscopy and morphological analysis

Micromasses at 3 weeks maturation were processed for transmission electron microscopy (TEM) and detailed cell viability analysis as previously described (8). Prior to thin sectioning, semi-thin sections were stained with 1% toluidine blue at 60°C, and observed by light microscopy for an overall specimen view, with particular reference to glycosaminoglycan(GAG)/proteoglycan content (8–10).

Cell viability analysis

In addition to TEM analysis, Tunel assays were done with an In situ Cell death Detection Kit (Roche). For some selected samples caspase 3 activity was assessed as previously described (11).

Confocal microscopy

Subcellular Sox9 distributions were analyzed by double immunofluorescence microscopy of 4% paraformaldehyde-fixed 5 μm sections of either micromass cultures or OA patient cartilage. Chondrocytes of middle zone cartilage were analyzed because their ECM microenvironment alterations are more akin to OA cartilage (12). Sox9 staining was done with 10 μg/ml goat anti-Sox9 polyclonal antibody (R&D), biotinylated bovine anti-goat antibody (3 μg/ml) (Jackson Laboratories, West Grove, PA) and a 1:400 dilution of Streptavidin Alexa Fluor 647 (Invitrogen, Carlsbad, CA). Control sections were scored with a normal goat IgG (10 μg/ml) primary antibody. Nuclei were counterstained with Sybr green (diluted 10,000 fold) (Invitrogen). Four fields of each of two sections from control or MMP-13 KD and IKKα KD micromasses were positioned along two orthogonal lines crossing the center with the highest Sox9 staining in the peripheral one third of each micromass. Streptavidin Alexa Fluor 647 labeled anti-Sox9 (rendered red) and Sybr green labeled DNA (rendered green) signals were co-localized by confocal imaging (details of the technique are in Supplementary Figure3's legend). Only sections passing through nuclei were submitted to confocal imaging. Sox9/DNA co-localized pixels appeared as yellow-orange with varying degrees of luminosity depending on the extent of co-localization.

Histochemical analysis

Micromasses were evaluated for glycosaminoglycan content by toluidine blue assay or scored for mineralized areas by alizarin red staining as previously described (5).

Western Blot analysis

Immunoblotting for specific proteins in monolayer and micromass cultures was performed with the same primary antibodies used for IHC or confocal microscopy. Total Proteins from ~1 e^5 cells were resolved on a 4–12% pre-cast gradient gel (Invitrogen), transferred to a PVDF membrane (Millipore). Signals were detected with appropriate secondary antibodies and revealed with an ECL Advance kit (Amersham, Little Chalfont, UK). Monoclonal anti-GAPDH (Chemicon) or anti-tubulin (Sigma) served as loading controls.

Statistics

All data are expressed as mean ± s.e.m. Non-parametric statistics were employed due to the small size of data sets as is typical for primary patient samples. Means of groups were

compared by Wilcoxon matched pairs test with CSS Statistical software (StatSoft, Tulsa, OK).

Results

Stable MMP-13 knock-down in populations of primary human OA chondrocytes

Primary ACs from independent OA human donors were stably transduced with moloney retroviruses harboring GL2 control or MMP-13 targeted shRNAs by puromycin selection. Real Time PCR analyses indicated strong KD efficiencies for two MMP-13 shRNAs targeted to different exons in (Figure 1A); and MMP-13 protein release was effectively blocked in either monolayer cultures (Figure 1B) or 3 week micromasses (Figure 1C) with or without exposure to IL-1β or other chemokines known to stimulate MMP-13 release.

MMP-13 KD blocked ECM remodeling and mineralization

Functional effects of MMP-13 in chondrocyte differentiation were analysed in micromass cultures in which ECM gradually gets remodelled and replaced by mineralized areas in conjunction with a loss in cell viability (5,8,10). MMP-13 KD prevented the loss of Col2 in 1–3 week micromass, not surprising given its predominant function in chondrocyte ECM remodelling. IHC analysis revealed enhanced Col2 accumulation in the absence of MMP-13 expression (Figure 2A and Supplemental Figure 1). C1,2C neo-epitopes, which are released by MMP cleavage from the carboxy-termini of Col2, were quantified in micromass cell supernatants by a sensitive ELISA based assay. Although no differences were observed between unstimulated control and MMP-13 KD micromass supernatants, MMP-13 KD strongly inhibited their release by cells in response to IL-1β or specific chemokines (Figure 2B) (albeit with some variation between different patients). C1,2C neo-epitopes in 1 week micromasses were only apparent in GL2 control but not in MMP-13 KD micromasses, as shown by in situ IHC and immunoblotting (Figure 2B).

Next we evaluated the effects of MMP-13 loss on the accumulation of ECM glycosaminoglycan (GAG). Quantitative DMMB biochemical assays revealed that MMP-13 KD micromasses had increased GAG content compared to their control counterparts (Figure 2C). The enhanced GAG deposition in MMP-13 KD samples was also confirmed by light microscopy observation of toluidine blue stained semithin sections (Figure 2C and Supplemental Figure 1). Calcium deposition was observed in 3 week control but not MMP13 KD micromasses by light microscopy (LM) visualization of alizarin red stained sections (Figure 2D and supplemental Figure 1).

MMP-13 ablation co-ordinately suppressed the expression and/or activities of effectors of chondrocyte differentiation including VEGF, Sox9, Runx2 and β-catenin and enhanced chondrocyte viability

To explore the mechanistic reasons for the lack of continued differentiation of MMP-13 null chondrocytes in both high density monolayer and micromass culture, we evaluated the expression of several pivotal regulatory proteins, which are responsible for chondrocyte differentiation towards a hypertrophic-like state including VEGF, Sox9, Runx2 and β-catenin. VEGF was suppressed at the mRNA level in MMP-13 KD chondrocyte monolayer and 1 week micromass and at the protein level by 3 weeks (Figure 3A and Supplemental Figure 1). Sox9 protein levels were highest in GL2 control monolayer cells and decreased during a 3 week time course in micromass cultures, as chondrocytes progressively became more differentiated. In contrast, Sox9 protein in MMP-13 KD monolayers was already lower than a matched GL2 positive control and these reduced Sox9 levels were stable over 3 weeks of micromass maturation (see IHC results in left panel of Figure 3B, other examples in Supplemental Figure 1, and their quantitative analysis in Supplemental Figure 2).

Immunoblotting of total cellular proteins also showed that Sox9 protein levels were reduced in monolayer and 1 week micromass cultures; and the latter was in keeping with blunted Sox9 mRNA levels in MMP-13 null monolayer and 1 week micromasses (Figure 3B, right panels). Runx2 protein, an essential positive regulator of chondrocyte maturation towards hypertrophy, progressively increased in GL2 control micromasses, while it remained at a constant low level in MMP-13 KD micromasses throughout the same time course (Figure 3C and Supplemental Figure 1). Reduced levels of Runx2 protein were also observed by immunoblotting of total cellular proteins of either high density monolayers or 3 week micromasses. Runx2 mRNA levels were also lower in MMP-13 KD monolayers and 1 week micromasses (Figure 3C).

Total β-catenin protein expression was higher in GL2 control micromasses compared to their MMP-13 KD counterparts (Figure 4A and IHC results of an independent patient's micromass in Supplemental Figure 1). β-catenin mRNA levels were reduced by MMP-13 ablation in monolayer and 1 week micromass cultures (Figure 4A); and levels of β-catenin protein were similarly blunted in immunoblots of total cellular proteins of both high density monolayer and 2 week micromass cultures. (Figure 4A) In addition, the active unphosphorylated form of β-catenin was present in 3 week GL2 micromasses by IHC and western blotting but was greatly reduced in the absence of MMP-13 (Figure 4B and Supplemental Figure 1). Interestingly, micromasses deficient for IKKα expression had similar reduced levels of active β-Catenin (see IHC and immunoblotting results in Figure 4B).

Importantly, the above inhibitory effects of MMP-13 ablation on several principal regulators of chondrocyte maturation towards a hypertrophic-like state occurred in conjunction with diminished Col10 expression (Figure 4C) and other changes in cellular physiology. Cellular viability was strongly enhanced by MMP-13 ablation as assessed by nuclear morphologies of GL2 control and MMP-13 KD micromasses prepared from multiple independent patients (see TEM images in Figure 4C). TEM also revealed that, unlike their matched GL2 controls, MMP-13 KD micromasses contained specialized cell-cell and cell-ECM junctions, integral nuclear and cytoplasmic membranes and healthy, elongated mitochondria replete with transverse septa indicative of a high metabolic rate (data not shown). These observations are also in keeping with the prolonged survival of growth plate chondrocytes in MMP-13 KO mice (4). Interestingly, the properties of MMP-13 KD micromass chondrocytes paralleled our prior observations in IKKα KD cells (8), in which MMP-13 activity was strongly suppressed in the absence of IKKα. Caspase 3 activity (reduction of 36% in two consecutive infections) and TUNEL staining agreed with these TEM ultrastructural observations (Figure 4C).

Loss of MMP13 or IKKα leads to the nuclear localization of Sox9

We employed confocal microscopy to analyze the effects of MMP-13 activity on Sox9 subcellular distribution (Figure 5). In all cases, the strongest Sox9 positive areas were found in the outer one third of micromasses, perhaps in part due to their asynchronous formation and intrinsic heterogeneity. Although MMP-13 KD micromasses expressed less Sox9 than their matched controls, higher levels of nuclear Sox9 were found in MMP-13 KD 1 week micromasses (see Figure 5A). The patterns of MMP-13 KD and GL2 micromasses differed markedly with only rare GL2 cells displaying a strong nuclear co-localization. Sox9 strongly stained most GL2 control nuclei in a halo-like manner, consistent with a peri-nuclear-like pattern at steady state (see Figure 5A, upper row and Supplemental Figure 3A). In contrast, MMP-13 KD cells presented a clear intranuclear Sox9 staining pattern with the GL2 control cells' nuclear halo-like pattern strikingly absent in all fields of view in the MMP-13 KD micromasses (see Figure 5A, middle row and Supplemental Figure 3B). Interestingly Sox9 subcellular distribution was strikingly similar in MMP-13 and IKKα KD cells suggesting

that their shared loss of MMP-13 activity had analogous consequences for the re-distribution of Sox9 (see Figure 5A, lower row and 3C). Noteworthy, akin to our GL2 control differentiated micromasses, middle zone chondrocytes in OA patient cartilage with extensively degraded ECM showed mostly peri-nuclear Sox9 staining (Figure 5B). In contrast chondrocytes in cartilage samples with stronger safranin-O staining, (indicative of more intact ECM), presented a mostly nuclear Sox9 staining pattern (Figure 5C), which resembled the sub-cellular Sox9 staining pattern of either MMP-13 or IKKα deficient chondrocytes in micromass cultures.

Discussion

MMP-13 functions in cartilage development

MMP-13 plays an important role at the hypertrophic stage of chondrocyte differentiation as they progress towards terminal endochondral ossification (13,14). Thus, because of MMP-13's important contribution to ECM remodeling preceding bone formation, only "temporary" not "permanent" articular cartilage expresses it; and MMP-13 mRNA is not significantly expressed in normal, maturation arrested human articular chondrocytes (15).

Three different MMP-13 KO mice have been described (3,4,16), which despite some phenotypic differences share a transient marked elongation of the hypertrophic chondrocyte zone. Conditional knock outs of MMP-13 in murine chondrocytes and osteoblasts revealed that cartilage ECM remodeling is the rate limiting process for hypertrophy triggering, terminal maturation, chondrocyte apoptosis and angiogenesis and osteoblast recruitment (4). The last Transverse Septa (LTS) are the critical active sites of matrix remodeling and collagen neo-epitope C1,2C accumulation due to MMP-13, there activated by MMP-14 expressed by neighboring osteoclasts (4). Above the LTS, hypertrophic, Col10 positive chondrocytes accumulate because their exit from the growth plate is delayed. Nonetheless, the absence of MMP-13 did not impede the conversion of proliferating chondrocytes into hypertrophic chondrocytes, most likely due to the auxiliary activity of other proteinases *in vivo* (MMP-9 and MMP-14) (4), which along with the contribution of neighboring osteoblasts, maintain ECM remodeling (14). On the other hand, transgenic postnatal expression of MMP-13 in articular cartilage caused chondrocyte hypertrophy along with Col10 induction (17).

Contribution of MMP-13 to OA disease

Functional connections between MMP-13 activity, pathological hypertrophic conversion and osteoarthritis have garnered considerable evidence from analysis of specimens derived from OA patients and *in vivo* animal models (16). Enforced MMP-13 transgene expression in hyaline cartilage resulted in progression to an OA-like pathology in adult mice (17). In keeping with that, impaired MMP-13 activity in TIMP3 knock-out mice caused evidence of a OA-like disease (18), with co-localized expresson of collagenase neo-epitopes and Col10. Moreover, MMP-13 expression also co-localizes with Col10 in the articular chondrocytes of adult mice subjected to surgically induced severe OA disease (19), indicative of articular cartilage in a hypertrophic-like state in spite of the fact that MMP-13 expression is normally absent in articular, maturation arrested ACs (16,19). On the other hand, MMP-13 ablation did not affect chondrocyte hypertrophy or osteophyte development at the articular cartilage level in a very recent report of an adult mouse model of surgically induced OA but did confer resistance to articular cartilage erosion (20).

A causative relationship between MMP-13 activity and chondrocyte hypertrophy has been reported in bovine cartilage explants following their exposure to a synthetic peptide fragment of Col2, which induced MMP-13 in conjunction with a hypertrophic-like

phenoype (21). A recent review has carefully detailed how biochemically different collagen fragments arising from different treatments act by triggering different catabolic pathways in the cells, and has also pointed out that differentiation related genes in articular cartilage are co-localized with focal areas of elevated Col2 degradation in OA cartilage (22).

In OA cartilage, the breakdown of normal cartilage homeostasis resembles at least to some degree the progression of chondrocytes from peri-articular to hypertrophic states in chondrogenesis. Normal healthy articular chondrocytes are stabilized in a “window” associated with a phenotype similar to that of periarticular chondrocytes, with a low level of Runx2 and an intermediate level of Sox9. Moreover, the enhanced Sox9 expression found in early passage OA chondrocytes compared to normal cartilage is part of the “OA fingerprint”, which appears to be partially retained during chondrocyte de-and re-differentiation *in vitro* (23). Thus, abnormal induction of MMP-13 in OA cartilage could act like a stress associated triggering event that relieves chondrocyte maturational arrest and facilitates their differentiation towards a hypertrophic-like state.

Micromasses prepared from primary articular chondrocytes recapitulate aspects of chondrocyte differentiation making them a convenient *in vitro* model for dissecting effectors that could also contribute to OA pathology (7,8,10,24). In this paper we have shown that MMP-13 ablation in micromass cultures stabilized their extracellular matrix, impaired chondrocyte terminal maturation and enhanced their viability and inhibited multiple effectors and regulators of chondrocyte differentiation. In this context we can not exclude the possibility that some of these effects of MMP13 loss could also in part be a consequence of altered processing of cytokines, receptors or other proteins.

MMP-13 is necessary for VEGF up-regulation

Healthy articular cartilage is an avascular tissue due to the activity of angiogenesis inhibitors secreted by chondrocytes, [reviewed in (25,26)], while osteochondral vascularity is associated with OA severity and clinical disease activity (25,26). VEGF, a major angiogenesis stimulator, has recently been shown to contribute to OA pathogenesis (27) and pellet cultures established from mouse MMP-13 KD chondrocytes have diminished angiogenic activities (28). Direct angiogenic activities of MMP-13 have also been previously noted (29) and MMP-13 may contribute to angiogenesis by releasing active VEGF from a complex with CTGF (30). Herein, our kinetic observations of maturing micromasses reveal that MMP-13 ablation prevents VEGF expression at both the protein and mRNA levels, suggesting that MMP-13 activity in this context contributes to VEGF up-regulation.

MMP-13 ablation affects the expression of multiple transcriptional regulators that differentially control terminal chondrocyte differentiation

Sox9 and Runx2 are pivotal transcription factors which interact in chondrocyte differentiation and exert opposing activities, so that their expression levels go in opposite directions across this process (31). While Sox9 maintains chondrocytes in a developmentally arrested state, Runx2 drives them to differentiate towards a hypertrophic-like state prior to ossification, [reviewed in (31)], which is also subject to additional complex regulation by the FGF, TGFβ, BMP and Wnt/β-catenin signaling pathways (32–36). Multiple lines of evidence support the notion that Wnt/β-catenin signalling pathways contribute to cartilage injury in OA (37). Over-expression of β-catenin in mice led to an OA like phenotype and OA patients show higher expression of β-catenin protein (36). β-catenin protein expression also parallels the onset of the disease in a spontaneous guinea pig osteoarthritis model (38). Wnt-16 and β-catenin are dramatically up-regulated in areas with moderate to severe OA compared to preserved cartilage areas (39). Canonical Wnt signaling promotes chondrocyte

differentiation and hypertrophy (40). In addition, phosphorylated β-catenin in Sox9 nuclear complexes was recently shown to be targeted for degradation (41).

Our observation of reduced Runx2 levels in MMP-13 KD chondrocytes are in agreement with other prior reports illustrating Runx2's pivotal role in terminal chondrocyte differentiation in endochondral ossification and OA disease by its regulatory links to MMP-13 and Col10. A carboxylate inhibitor of MMP-13 strongly suppressed Runx2 mRNA levels in conjunction with losses in Col2 degradation, calcium deposition and Col10 expression in pre-hypertrophic, bovine fetal growth plate chondrocytes cultured at high density (42). Thus, Runx2 has common functional roles in articular (this paper) or growth plate chondrocyte maturation (42) with respect to MMP-13 dependent ECM remodelling. In addition, the murine (43) and human (44) *ColX* genes are also direct Runx2 transcriptional targets; and accordingly Runx2 deficient mice have profound deficits in Col10 expression. Importantly, Runx-2 also controls murine AC differentiation towards hypertrophy *in vivo* in an OA inductive surgery model, wherein Runx-2 deficient mice exhibited decreased cartilage destruction and osteophyte formation and reduced levels of MMP-13 and Col10 (45).

Evidence that MMP-13 activity is linked to the Sox9 dependent control of β-catenin

Confocal microscopy experiments revealed that MMP-13 and IKKα strongly influence the subcellular localization of Sox9. Sox9 exhibited a mostly peri-nuclear staining pattern in control differentiated micromasses, but in contrast it localized mostly within nuclei of MMP-13 and IKKα deficient chondrocyte micromasses (Figure 5 and Supplemental Figure 3). Moreover, we also found that Sox9 localized to the nuclei of middle zone chondrocytes in samples of OA cartilage with intact ECM but was mostly excluded from nuclear entry in chondrocytes in OA cartilage with extensively degraded ECM (Figure 5). An apparent discrepancy with an earlier study (46) can be explained by differences in the sensitivities and resolution of our confocal microscopy protocol and also because we focused on middle zone chondrocytes.

Interestingly Sox9 nuclear localization inversely correlated with β-catenin stability and activation status (Figure 4 and Suppl. Figure 1). Sox9 was previously shown to inhibit β-catenin dependent signalling not only in chondrocytes (47) but also in the intestinal epithelium (48). In keeping with our observations, a more recent report also demonstrated that enhanced nuclear levels of Sox9 can directly lead to β-catenin degradation (41) by stabilization of GSK-3β, an essential component of the β-catenin degradation complex. Interestingly, the reduced level of VEGF mRNA in our MMP-13 KD micromasses would also be consistent with their deficit in active β-catenin, since VEGF is a β-Catenin target gene [reviewed in (49)]. However, despite our finding of enhanced nuclear Sox-9 accumulation in MMP-13 KD micromasses, gene expression arrays have not revealed evidence of increased levels of Sox9 target gene mRNAs (data not shown), suggesting that different nuclear Sox9 levels are required to manifest its independent inhibitory and activating functions. Moreover in further agreement with our observation linking enhanced nuclear levels of Sox9 with VEGF suppression, besides interfering with β-catenin activation, Sox9 was also recently reported to directly suppress VEGF expression by binding to SRY sites in the *Vegfa* gene (50). However and importantly, VEGF levels are elevated in the growth plate, due to Sox9 down-regulation at that site, which is also necessary for endochondral ossification (50).

Based of our collective findings, we propose that MMP-13 dependent ECM remodelling, in differentiating chondrocyte micromass cultures or in cartilage disease states such as OA, pushes chondrocytes out of their natural homeostasis towards a hypertrophic-like state by

having effects on a combination of regulatory factors (including Runx2, Sox9, β-Catenin and VEGF) that act in concert to drive terminal chondrocyte differentiation.

Supplementary Material

Refer to Web version on PubMed Central for supplementary material.

Acknowledgments

This work was supported by the Rizzoli Institute, the Carisbo Foundation (EO, RV and SP), a MIUR 40% Grant (FF, EF and AF), a Rientro dei Cervelli award (AF and KBM), the MAIN EU FPVI Network of Excellence (OE, MP and KBM), USA NIH grant GM066882 (awarded to KBM), and a Progetto Strategico di Ateneo award. KBM was a senior scholar of the Institute of Advanced Studies of the University of Bologna at the onset of this work. The authors declare no conflicting financial interests.

Contract grant sponsor: CARISBO Foundation; Contract grant number: 2005-1059;

Contract grant sponsor: Ricerca Corrente Istituti Ortopedici Rizzoli, Bologna, Italy.

References

1. Drissi H, Zuscik M, Rosier R, O'Keefe R. Transcriptional regulation of chondrocyte maturation: potential involvement of transcription factors in OA pathogenesis. Mol Aspects Med. 2005; 26(3): 169–79. [PubMed: 15811433]
2. Ortega N, Behonick DJ, Werb Z. Matrix remodeling during endochondral ossification. Trends Cell Biol. 2004; 14(2):86–93. [PubMed: 15102440]
3. Inada M, Wang Y, Byrne MH, Rahman MU, Miyaura C, Lopez-Otin C, et al. Critical roles for collagenase-3 (Mmp13) in development of growth plate cartilage and in endochondral ossification. Proc Natl Acad Sci U S A. 2004; 101(49):17192–7. [PubMed: 15563592]
4. Stickens D, Behonick DJ, Ortega N, Heyer B, Hartenstein B, Yu Y, et al. Altered endochondral bone development in matrix metalloproteinase 13-deficient mice. Development. 2004; 131(23): 5883–95. [PubMed: 15539485]
5. Olivotto E, Vitellozzi R, Fernandez P, Falcieri E, Battistelli M, Burattini S, et al. Chondrocyte hypertrophy and apoptosis induced by GROalpha require three-dimensional interaction with the extracellular matrix and a co-receptor role of chondroitin sulfate and are associated with the mitochondrial splicing variant of cathepsin B. J Cell Physiol. 2007; 210(2):417–27. [PubMed: 17096385]
6. Vincenti MP, Brinckerhoff CE. Transcriptional regulation of collagenase (MMP-1, MMP-13) genes in arthritis: integration of complex signaling pathways for the recruitment of gene-specific transcription factors. Arthritis Res. 2002; 4(3):157–64. [PubMed: 12010565]
7. Gerstenfeld LC, Landis WJ. Gene expression and extracellular matrix ultrastructure of a mineralizing chondrocyte cell culture system. J Cell Biol. 1991; 112(3):501–13. [PubMed: 1991793]
8. Olivotto E, Borzi RM, Vitellozzi R, Pagani S, Facchini A, Battistelli M, et al. Differential requirements for IKKalpha and IKKbeta in the differentiation of primary human osteoarthritic chondrocytes. Arthritis Rheum. 2008; 58(1):227–39. [PubMed: 18163512]
9. Battistelli M, Borzi RM, Olivotto E, Vitellozzi R, Burattini S, Facchini A, et al. Cell and matrix morpho-functional analysis in chondrocyte micromasses. Microsc Res Tech. 2005; 67(6):286–95. [PubMed: 16173090]
10. Hyllested JL, Veje K, Ostergaard K. Histochemical studies of the extracellular matrix of human articular cartilage--a review. Osteoarthritis Cartilage. 2002; 10(5):333–43. [PubMed: 12027534]
11. Facchini A, Borzi RM, Marcu KB, Stefanelli C, Olivotto E, Goldring MB, et al. Polyamine depletion inhibits NF-kappaB binding to DNA and interleukin-8 production in human chondrocytes stimulated by tumor necrosis factor-alpha. J Cell Physiol. 2005; 204(3):956–63. [PubMed: 15828019]

12. Sandell LJ, Aigner T. Articular cartilage and changes in arthritis. An introduction: cell biology of osteoarthritis. Arthritis Res. 2001; 3(2):107–13. [PubMed: 11178118]
13. van der Kraan PM, van den Berg WB. Osteoarthritis in the context of ageing and evolution. Loss of chondrocyte differentiation block during ageing. Ageing Res Rev. 2008; 7(2):106–13. [PubMed: 18054526]
14. Malemud CJ. Matrix metalloproteinases: role in skeletal development and growth plate disorders. Front Biosci. 2006; 11:1702–15. [PubMed: 16368549]
15. Bau B, Gebhard PM, Haag J, Knorr T, Bartnik E, Aigner T. Relative messenger RNA expression profiling of collagenases and aggrecanases in human articular chondrocytes in vivo and in vitro. Arthritis Rheum. 2002; 46(10):2648–57. [PubMed: 12384923]
16. Takaishi H, Kimura T, Dalal S, Okada Y, D'Armiento J. Joint diseases and matrix metalloproteinases: a role for MMP-13. Curr Pharm Biotechnol. 2008; 9(1):47–54. [PubMed: 18289056]
17. Neuhold LA, Killar L, Zhao W, Sung ML, Warner L, Kulik J, et al. Postnatal expression in hyaline cartilage of constitutively active human collagenase-3 (MMP-13) induces osteoarthritis in mice. J Clin Invest. 2001; 107(1):35–44. [PubMed: 11134178]
18. Sahebjam S, Khokha R, Mort JS. Increased collagen and aggrecan degradation with age in the joints of Timp3(−/−) mice. Arthritis Rheum. 2007; 56(3):905–9. [PubMed: 17328064]
19. Kamekura S, Hoshi K, Shimoaka T, Chung U, Chikuda H, Yamada T, et al. Osteoarthritis development in novel experimental mouse models induced by knee joint instability. Osteoarthritis Cartilage. 2005; 13(7):632–41. [PubMed: 15896985]
20. Little CB, Barai A, Burkhardt D, Smith SM, Fosang AJ, Werb Z, et al. Matrix metalloproteinase 13-deficient mice are resistant to osteoarthritic cartilage erosion but not chondrocyte hypertrophy or osteophyte development. Arthritis & Rheumatism. 2009; 60(12):3723–3733. [PubMed: 19950295]
21. Tchetina EV, Kobayashi M, Yasuda T, Meijers T, Pidoux I, Poole AR. Chondrocyte hypertrophy can be induced by a cryptic sequence of type II collagen and is accompanied by the induction of MMP-13 and collagenase activity: implications for development and arthritis. Matrix Biol. 2007; 26(4):247–58. [PubMed: 17306969]
22. Gauci SJ, Golub SB, Tutolo L, Little CB, Sims NA, Lee ER, et al. Modularing chondrocyte hypertrophy in growth plate and osteoarthritic cartilage. J Musculoskelet Neuronal Interact. 2008; 8(4):308–310. [PubMed: 19147951]
23. Yang KG, Saris DB, Geuze RE, van Rijen MH, van der Helm YJ, Verbout AJ, et al. Altered in vitro chondrogenic properties of chondrocytes harvested from unaffected cartilage in osteoarthritic joints. Osteoarthritis Cartilage. 2006; 14(6):561–70. [PubMed: 16735197]
24. Zhang Z, McCaffery JM, Spencer RG, Francomano CA. Hyaline cartilage engineered by chondrocytes in pellet culture: histological, immunohistochemical and ultrastructural analysis in comparison with cartilage explants. J Anat. 2004; 205(3):229–37. [PubMed: 15379928]
25. Bonnet CS, Walsh DA. Osteoarthritis, angiogenesis and inflammation. Rheumatology (Oxford). 2005; 44(1):7–16. [PubMed: 15292527]
26. Walsh DA, Bonnet CS, Turner EL, Wilson D, Situ M, McWilliams DF. Angiogenesis in the synovium and at the osteochondral junction in osteoarthritis. Osteoarthritis Cartilage. 2007; 15(7): 743–51. [PubMed: 17376709]
27. Murata M, Yudoh K, Masuko K. The potential role of vascular endothelial growth factor (VEGF) in cartilage: how the angiogenic factor could be involved in the pathogenesis of osteoarthritis? Osteoarthritis Cartilage. 2008; 16(3):279–86. [PubMed: 17945514]
28. Kosaki N, Takaishi H, Kamekura S, Kimura T, Okada Y, Minqi L, et al. Impaired bone fracture healing in matrix metalloproteinase-13 deficient mice. Biochem Biophys Res Commun. 2007; 354(4):846–51. [PubMed: 17275784]
29. Zijlstra A, Aimes RT, Zhu D, Regazzoni K, Kupriyanova T, Seandel M, et al. Collagenolysis-dependent angiogenesis mediated by matrix metalloproteinase-13 (collagenase-3). J Biol Chem. 2004; 279(26):27633–45. [PubMed: 15066996]

30. Hashimoto G, Inoki I, Fujii Y, Aoki T, Ikeda E, Okada Y. Matrix metalloproteinases cleave connective tissue growth factor and reactivate angiogenic activity of vascular endothelial growth factor 165. J Biol Chem. 2002; 277(39):36288–95. [PubMed: 12114504]

31. Goldring MB, Tsuchimochi K, Ijiri K. The control of chondrogenesis. J Cell Biochem. 2006; 97(1):33–44. [PubMed: 16215986]

32. Haque T, Nakada S, Hamdy RC. A review of FGF18: Its expression, signaling pathways and possible functions during embryogenesis and post-natal development. Histol Histopathol. 2007; 22(1):97–105. [PubMed: 17128416]

33. Wu X, Shi W, Cao X. Multiplicity of BMP signaling in skeletal development. Ann N Y Acad Sci. 2007; 1116:29–49. [PubMed: 18083919]

34. Yoon BS, Pogue R, Ovchinnikov DA, Yoshii I, Mishina Y, Behringer RR, et al. BMPs regulate multiple aspects of growth-plate chondrogenesis through opposing actions on FGF pathways. Development. 2006; 133(23):4667–78. [PubMed: 17065231]

35. Zhong N, Gersch RP, Hadjiargyrou M. Wnt signaling activation during bone regeneration and the role of Dishevelled in chondrocyte proliferation and differentiation. Bone. 2006; 39(1):5–16. [PubMed: 16459154]

36. Zhu M, Tang D, Wu Q, Hao S, Chen M, Xie C, et al. Activation of beta-Catenin Signaling in Articular Chondrocytes Leads to Osteoarthritis-Like Phenotype in Adult beta-Catenin Conditional Activation Mice. J Bone Miner Res. 2009; 24(1):12–21. [PubMed: 18767925]

37. Corr M. Wnt-beta-catenin signaling in the pathogenesis of osteoarthritis. Nat Clin Pract Rheumatol. 2008; 4(10):550–6. [PubMed: 18820702]

38. Yuasa T, Otani T, Koike T, Iwamoto M, Enomoto-Iwamoto M. Wnt/beta-catenin signaling stimulates matrix catabolic genes and activity in articular chondrocytes: its possible role in joint degeneration. Lab Invest. 2008; 88(3):264–74. [PubMed: 18227807]

39. Dell'accio F, De Bari C, Eltawil NM, Vanhummelen P, Pitzalis C. Identification of the molecular response of articular cartilage to injury, by microarray screening: Wnt-16 expression and signaling after injury and in osteoarthritis. Arthritis Rheum. 2008; 58(5):1410–21. [PubMed: 18438861]

40. Yano F, Kugimiya F, Ohba S, Ikeda T, Chikuda H, Ogasawara T, et al. The canonical Wnt signaling pathway promotes chondrocyte differentiation in a Sox9-dependent manner. Biochem Biophys Res Commun. 2005; 333(4):1300–8. [PubMed: 15979579]

41. Topol L, Chen W, Song H, Day TF, Yang Y. Sox9 inhibits Wnt signaling by promoting beta-catenin phosphorylation in the nucleus. J Biol Chem. 2009; 284(5):3323–33. [PubMed: 19047045]

42. Wu CW, Tchetina EV, Mwale F, Hasty K, Pidoux I, Reiner A, et al. Proteolysis involving matrix metalloproteinase 13 (collagenase-3) is required for chondrocyte differentiation that is associated with matrix mineralization. J Bone Miner Res. 2002; 17(4):639–51. [PubMed: 11918221]

43. Zheng Q, Zhou G, Morello R, Chen Y, Garcia-Rojas X, Lee B. Type X collagen gene regulation by Runx2 contributes directly to its hypertrophic chondrocyte-specific expression in vivo. J Cell Biol. 2003; 162(5):833–842. [PubMed: 12952936]

44. Higashikawa A, Saito T, Ikeda T, Kamekura S, Kawamura N, Kan A, et al. Identification of the core element responsive to runt-related transcription factor 2 in the promoter of human type x collagen gene. Arthritis & Rheumatism. 2009; 60(1):166–178. [PubMed: 19116917]

45. Kamekura S, Kawasaki Y, Hoshi K, Shimoaka T, Chikuda H, Maruyama Z, et al. Contribution of runt-related transcription factor 2 to the pathogenesis of osteoarthritis in mice after induction of knee joint instability. Arthritis Rheum. 2006; 54(8):2462–70. [PubMed: 16868966]

46. Aigner T, Gebhard PM, Schmid E, Bau B, Harley V, Poschl E. SOX9 expression does not correlate with type II collagen expression in adult articular chondrocytes. Matrix Biol. 2003; 22(4):363–72. [PubMed: 12935820]

47. Akiyama H, Lyons JP, Mori-Akiyama Y, Yang X, Zhang R, Zhang Z, et al. Interactions between Sox9 and beta-catenin control chondrocyte differentiation. Genes Dev. 2004; 18(9):1072–87. [PubMed: 15132997]

48. Bastide P, Darido C, Pannequin J, Kist R, Robine S, Marty-Double C, et al. Sox9 regulates cell proliferation and is required for Paneth cell differentiation in the intestinal epithelium. J Cell Biol. 2007; 178(4):635–48. [PubMed: 17698607]

49. Pishvaian MJ, Byers SW. Biomarkers of WNT signaling. Cancer Biomarkers. 2007; 3(4):263–274. [PubMed: 17917155]

50. Hattori T, Muller C, Gebhard S, Bauer E, Pausch F, Schlund B, et al. SOX9 is a major negative regulator of cartilage vascularization, bone marrow formation and endochondral ossification. Development. 2010; 137(6):901–911. [PubMed: 20179096]

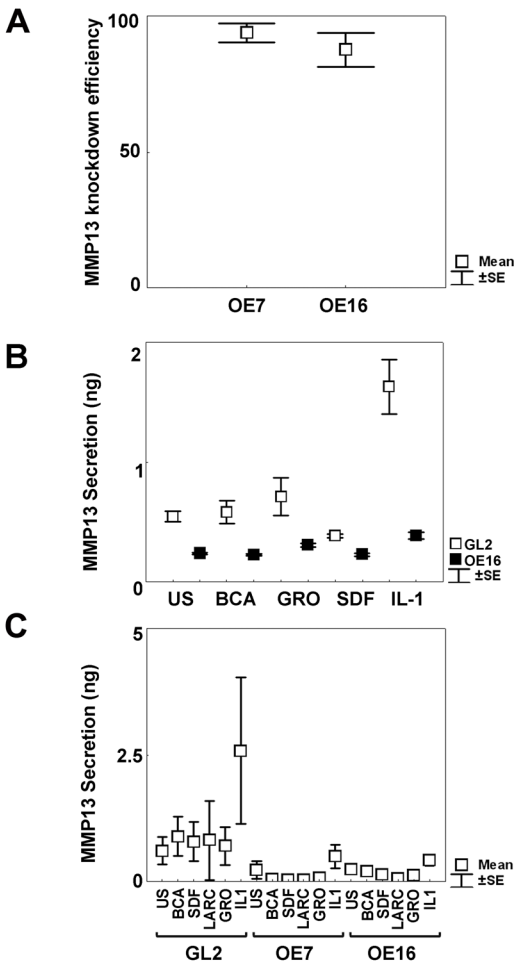

Figure 1. Stable knock-down (KD) of MMP-13 expression by retroviral transduction

A. Real time PCR verification of MMP-13 KD by shOligos targeted to different MMP-13 exons. The loss of MMP-13 expression (mean percentage KD±SEM) were as follows: OE7 (3 patients) 91%±3.8; OE16 (6 patients): 83.1%±10,5. **B.** One representative experiment out of three different patients'chondrocytes tested in triplicate wells, where KD efficiencies were quantified by MMP-13 ELISA assay of cell supernatants in unstimulated or stimulated conditions with 100 nM chemokines (BCA, GROα, SDF) or 100 units/ml IL-1β for 72 hours. **C.** 3 week micromasses were left unstimulated or stimulated with 100 nM chemokines (BCA, SDF, Larc, GROα) or 100 units/ml IL-1β for 72 hours. MMP-13 KD statistically decreased MMP-13 release from IL-1 stimulated OE16 micromasses (p=0.046). Results were obtained from duplicate micromass cultures of 6 different patients.

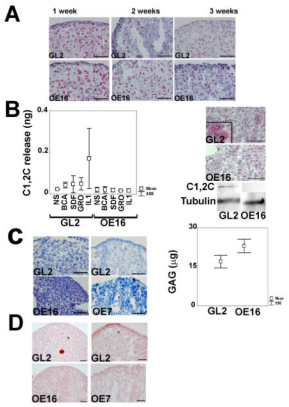

Figure 2. Effects of MMP-13 ablation on ECM remodeling, chondrocyte terminal differentiation and mineralization

A. Col2 IHC analysis across a micromass maturation time course of 1–3 weeks (bar = 50 μm); **B**. Left side: ELISA assays for release of type II collagen C1,2C neo-epitopes into 3 week micromass supernatants in response to MMP-13 inductive stimuli. Results were obtained from two different patients (mean+/−SEM); **B.** Right side: IHC staining and western blotting of C1,2C neo-epitopes in control vs. MMP-13 KD micromasses (1 w); **C.** Left side: Example of toluidine blue staining for GAG/proteoglycan in control vs. MMP-13 KD (OE16 and OE7) micromasses (3 w) (bar = 50 μm); **C.** Right side: Cumulative data from 5 different patients of quantitative DMMB assay for sulphated GAG accumulation in controls vs. MMP-13 KD micromasses (3 w). MMP-13 KD micromasses had statistically higher GAG (μg) content compared to control micromasses ($p= 0.012$). **D.** Alizarin red staining for calcium deposition in control vs. MMP-13 KD (OE16 and OE7) micromasses (3 w).

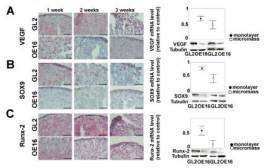

Figure 3. Effects of MMP-13 loss on VEGF and multiple transcriptional regulators of chondrocyte diffentiation in maturing (1–3 week) micromasses

A. Left side: VEGF IHCs of GL2 control vs. MMP13-KD micromass cultures (bar = 50 μm). **A.** Right side: levels (mean±SEM) of VEGF mRNA, relative to matched GL2 control mRNA, in high density monolayer (5 patients, with p=0.043) and 1-week micromasses (4 patients, empty boxes); VEGF western blot of high density monolayer and micromasses (3 w); **B.** Left side: Sox9 IHC of GL2 and MMP-13 KD micromass (bar = 50 μm). **B.** Right side: levels (mean±SEM) of Sox9 mRNA, relative to matched GL2 control mRNA, in high density monolayer (6 patients, significant difference at p=0.028) and 1-week micromasses (4 patients); Sox-9 western blots of control and MMP-13 KD high density monolayer and micromasses (1 w); **C.** Left side: Runx2 IHC of GL2 and MMP13-KD micromasses (bar = 50μM). **C.** Right side: levels (mean±SEM) of Runx2 mRNA, in MMP-13 KD samples relative to matched GL2 controls, in high density monolayer (5 patients, significant difference at p=0.043) and 1-week micromasses (2 patients); Runx2 immunoblots of control and MMP-13 KD high density monolayer and micromasses at 3 weeks.

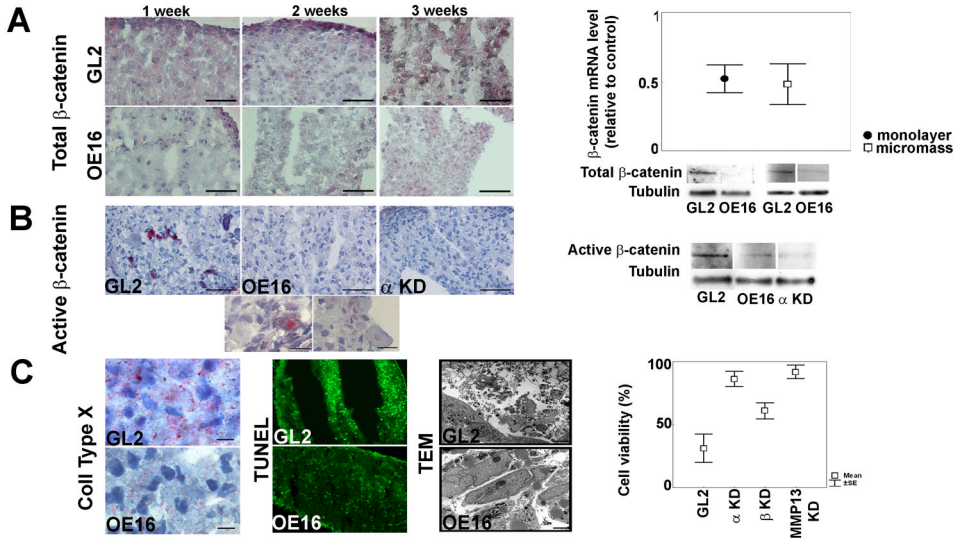

Figure 4. Effects of MMP-13 ablation on β catenin expression and activation, hypertrophy and cell viability

A. (Left): β-catenin IHCs of GL2 and MMP-13 in differentiating micromasses (bar = 50 μm); **A** (Right): β-catenin mRNA levels (mean±SEM) in MMP-13 KD vs. matched GL2 controls, in high density monolayer (5 patients, p=0.043) and 1 week (w) micromasses (5 patients, p=0.043). Immunoblots of β-catenin in control vs. MMP-13 KD high density monolayer and micromasses (2w); **B** (Left): Activated β-catenin in GL2, MMP-13 KD and IKKα KD 3w micromasses (bar =50 μm). Higher magnification GL2 images (bar=12.5 μm) reveal nuclear activated β-catenin and hypertrophic chondrocyte morphology (larger size and lower nuclear/cytoplasmic index); **B** (Right): Immunoblots of active β-catenin in GL2 control vs. MMP-13 KD and IKKα KD micromasses (3w); **C** (Left): Collagen X IHC (3w, bar = 18.7 μm), TUNEL fluorescence (2w) and cell morphology by TEM (3w, bar = 2 μm) in GL2 vs. MMP-13 KD micromasses; **C** (Right): TEM analysis of nuclear morphology and integrity in MMP-13 KD, IKKα KD and IKKβ KD micromasses (5 patients each). MMP-13 KD significantly increases chondrocyte viability over GL2 control micromasses (p= 0.043).

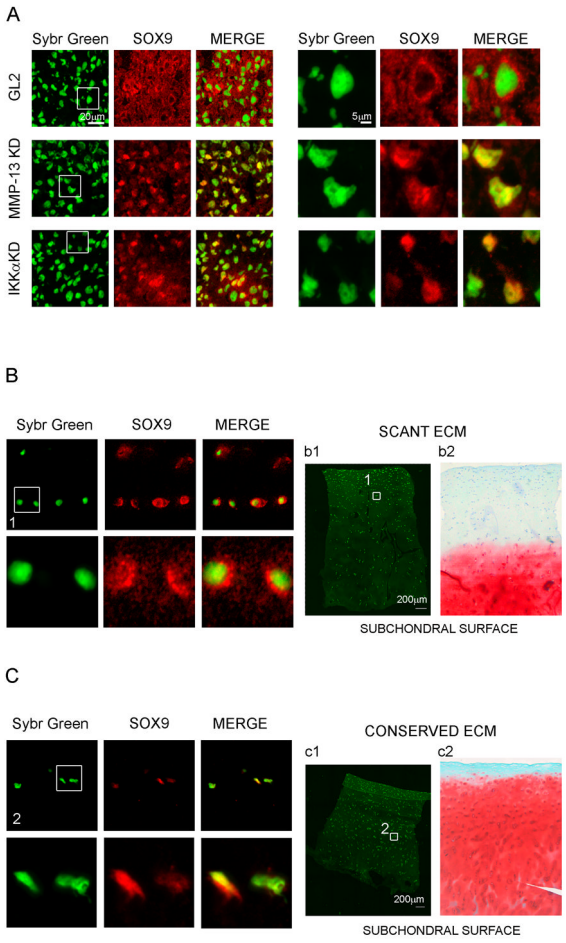

Figure 5. Sox9 subcellular localization in micromasses with and without MMP-13 and IKKα expression and in cartilage tissues with scant vs. more intact ECM

Confocal microscopy analysis of Sox9 subcellular distribution in 1 week micromasses: Sybr Green nuclear staining, Sox9 staining, and merge. Areas identified by the white square are shown at higher magnification on the right (original images were acquired with a 40× objective in the left panels, and with a 60× in the right panels). Upper row: GL2 control micromasses; middle row: MMP-13 KD micromasses; lower row: IKKα KD micromasses. **B and C**: Confocal analysis of Sox9 subcellular distribution in the middle zone chondrocytes of degraded cartilage (**B**) and conserved cartilage (**C**) (40× and 60× magnifications are shown). The areas of cartilage used for confocal acquisition of scant or conserved cartilage are shown in panels b1 and c1 (sybr green staining only), respectively. Panels b2 and c2 show safranin-O staining in consecutive sections of the same samples used for confocal analysis.